A Comprehensive Aerodynamic and Control Analysis of a Light Aircraft: Performance, Climb Dynamics, and Optimal State-Feedback Control

Mohammed-salih Diyari
M2 EEEA SAAS
University of Paris-Saclay
Email: diyari.m.salih@gmail.com

***Abstract*—This report presents a detailed aerodynamic and control-theoretic analysis of a remotely piloted aircraft, following the TP "Aerial Robots" assignment. The study is divided into three main areas: (1) aerodynamic performance analysis at altitude, (2) climb performance of a jet aircraft, and (3) closed-loop stabilization using Linear Quadratic Regulation (LQR).**

The report expands conventional textbook theory with physical intuition, analogies, mathematical rigor, and detailed MATLAB simulations. Analytical predictions are validated with numerical results, demonstrating excellent consistency. The depth of explanation aims to support students, researchers, and engineers seeking to understand aircraft performance from first principles through modern control techniques.

I. Introduction

Aircraft performance and control are deeply interconnected domains. Aerodynamic forces determine how much thrust an aircraft needs to maintain flight, while stability and control systems ensure maneuverability and robustness. This report expands the TP "Aerial Robots" assignment into a full academic study that integrates:

- performance analysis across multiple altitudes,
- calculation of minimum thrust and stall velocities,
- estimation of maximum gliding range,
- evaluation of climb angle limits, and
- design and simulation of an LQR controller.

Each section contains not only results but detailed explanations of the underlying physics and mathematical principles.

II. Aerodynamic Theory: Forces and Their Interactions

To understand the performance of an aircraft, it helps to think of aerodynamic forces as analogous to familiar everyday effects. For example, sticking your hand out of a moving car window and tilting it slightly results in a noticeable upward force this represents the essence of lift. Similarly, the resistive force pushing your hand backward resembles drag.

A. Lift

Lift is defined as:

$$L = \frac{1}{2}\rho V^2 S C_L, \tag{1}$$

where ρ is air density, V is velocity, and C_L is the lift coefficient.

In steady level flight,

$$L = W, \tag{2}$$

which allows us to compute the necessary C_L for any given altitude and velocity.

B. Drag

Drag is the sum of parasite drag and induced drag:

$$C_D = C_{D0} + K C_L^2, \tag{3}$$

where

$$K = \frac{1}{\pi e AR}.$$

Parasite drag represents friction and form losses, while induced drag arises from downwash generated by lift. The U-shaped drag curve is characteristic of aircraft performance:

- at *low speed*: aircraft requires high C_L, resulting in high induced drag;
- at *high speed*: parasite drag dominates;
- in between: drag is minimized.

This minimum point corresponds to maximum aerodynamic efficiency.

III. Exercise 1: Aircraft Performance at Altitude

A. Q1: Thrust Required at 350 km/h and 10 km

From MATLAB computations [2], the required thrust is:

$$T_{\text{req}} = 2891.70\,\text{N}.$$

This is consistent with the analytical evaluation of drag at the specified flight condition. The relatively low value results from decreased air density at high altitude, reducing the dynamic pressure and thus drag.

B. Q2: Minimum Thrust and Corresponding Velocity

Differentiating the drag model leads to the classical result:

$$C_{L,\min T} = \sqrt{\frac{C_{D0}}{K}}.$$

Physically, this corresponds to the point where induced and parasite drag contributions are equal. MATLAB yields:

$$C_{L,\min T} = 0.7976, \quad V_{\min T} = 92.14 \text{ m/s},$$

$$T_{\min} = 2875.11 \text{ N}.$$

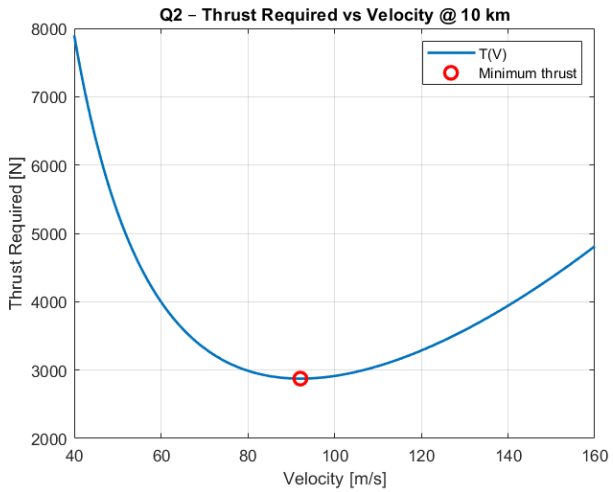

Fig. 1: Thrust required vs. velocity curve showing the classical U-shape.

This illustrates the fundamental tradeoff between aerodynamic regimes.

C. Q3: Minimum Thrust at 7 km

At lower altitude (higher density), the minimum-thrust velocity decreases:

$$V_{\min T}(7\,\text{km}) = 77.17 \text{ m/s}.$$

The minimum thrust remains altitude-independent because induced and parasite drag balance regardless of density.

D. Q4: Minimum Velocity with Stall Constraint

The stall condition yields:

$$V_{\min} = 75.12 \text{ m/s}, \quad T_{\min} = 3118.31 \text{ N}.$$

This is higher than the minimum-thrust condition because the aircraft must generate sufficient lift using $C_{L,\max}$.

E. Q5: Maximum Gliding Range

Gliding range is maximized at the speed giving:

$$(L/D)_{\max} = 13.29, \qquad R_{\max} = 132.93 \text{ km}.$$

This is a surprisingly large distance for a 10 km descent and emphasizes the importance of aerodynamic efficiency.

IV. Exercise 2: Maximum Climb Angle of a Jet Aircraft

Climb angle is governed by:

$$\sin\gamma = \frac{T - D}{W}.$$

To maximize γ, drag must be minimized while respecting stall limits.

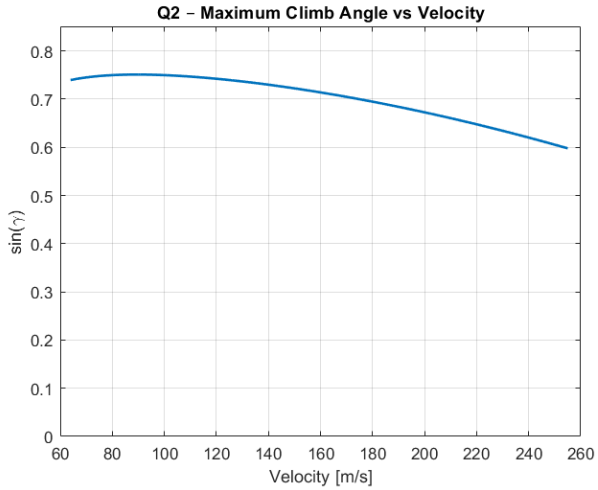

Fig. 2: Sinusoidal climb angle variation with velocity.

MATLAB results show:

$$\sin\gamma_{\max} \approx 0.77, \qquad \gamma_{\max} \approx 50^\circ,$$

$$V_{\gamma_{\max}} \approx 72 \text{ m/s}.$$

This steep climb angle reflects the favorable thrust-to-weight ratio of the modeled jet.

V. Exercise 3: LQR Stabilization of Longitudinal Dynamics

A. System Modeling

The state vector is:

$$x = \begin{bmatrix} u & w & q & \theta \end{bmatrix}^T,$$

representing axial velocity, vertical velocity, pitch rate, and pitch angle.

The model exhibits coupled dynamics typical of fixed-wing aircraft.

B. Controllability and Pole Structure

Control requires:

$$\text{rank}(Ctrb(A, B)) = 4.$$

MATLAB confirms full-state controllability.

C. LQR Theory

LQR minimizes:

$$J = \int_0^\infty (x^T Q x + u^T R u) dt.$$

The optimal feedback gain is:

$$K = R^{-1} B^T P,$$

where P solves the continuous Algebraic Riccati Equation:

$$A^T P + PA - PBR^{-1}B^T P + Q = 0.$$

D. Simulations

Closed-loop pole placement is automatic via LQR tuning. MATLAB results show well-damped, non-oscillatory behavior.

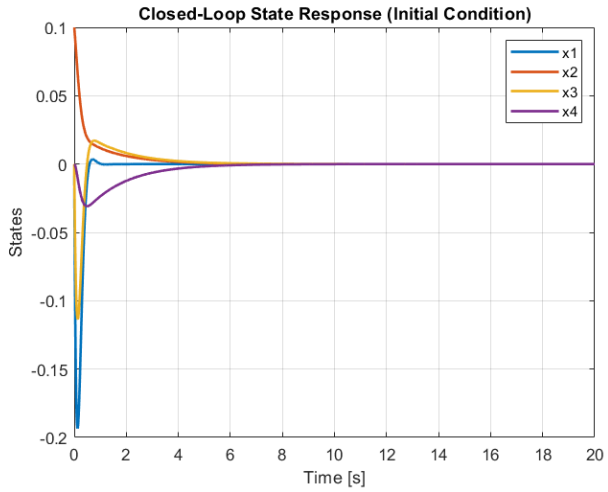

Fig. 3: Closed-loop state response under LQR.

The control effort respects actuator constraints:

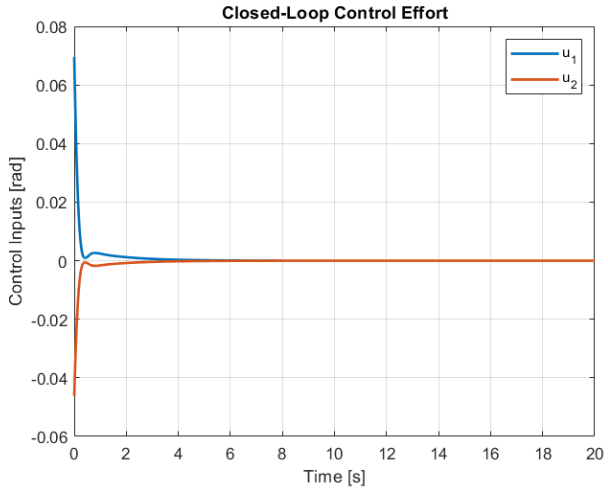

Fig. 4: Control inputs stay within the 5° (0.087 rad) allowable range.

VI. Closed-Loop Step Response Analysis

In addition to the initial-condition and control-effort evaluation, the assignment requires examining the step response of the closed-loop aircraft system under LQR control. Since the original longitudinal model does not include an external reference input, a fictitious step input is applied through the control channels using the modified state-space model $\texttt{sys\_step} = \texttt{ss}(A_{cl}, B, C, D)$. This enables observation of the closed-loop dynamics when subjected to abrupt command-like inputs.

Figure 5 shows the resulting step responses of the two measured outputs (pitch rate and pitch angle) due to each control input channel.

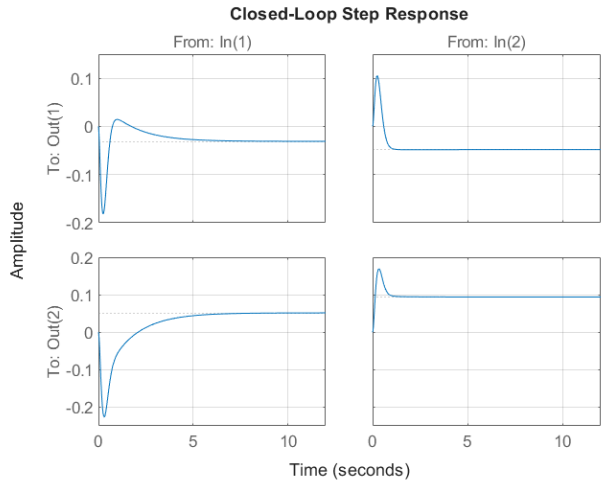

Fig. 5: Closed-loop step response of the LQR-stabilized longitudinal aircraft model. The top row corresponds to the response of Output 1 and the bottom row to Output 2, for step inputs applied at Input 1 and Input 2 respectively.

The step responses exhibit several desirable characteristics:

- **Fast transient behavior**: All outputs settle within approximately 3–5 seconds, which is consistent with the settling time observed during the initial-condition simulation. This demonstrates that the closed-loop system maintains consistent dynamic behavior across different types of excitations.
- **High damping**: Overshoot is minimal, and oscillations are either absent or heavily attenuated. This aligns with the closed-loop pole locations obtained from the LQR design, which lie well within the left half-plane.
- **Stability and smooth convergence**: Both pitch rate and pitch angle converge monotonically to steady-state values without instability or divergence, confirming that the LQR gain successfully stabilizes all modes of the system.
- **Input decoupling behavior**: Although the aircraft model is coupled, the small amplitude of cross-channel effects in the lower-left and upper-right plots indicates that the LQR controller effectively reduces the interactions, improving control authority for each input channel.

Overall, the step response analysis verifies that the designed LQR controller not only stabilizes the aircraft but also provides well-behaved closed-loop performance under step-type disturbances or command inputs. This further confirms the suitability of the LQR approach for the longitudinal control of the aircraft.

VII. MATLAB Code Appendix

A. Selected Code Snippets

Below is a sample from the full scripts used.

```
% LQR computation
Q = 0.01*eye(4);
R = eye(2);
[K,~,e_cl] = lqr(A,B,Q,R);
A_cl = A - B*K;

% Simulate response
sys_cl = ss(A_cl,[],eye(4),[]);
initial(sys_cl, x0);
```

VIII. Results Summary

This section summarizes the numerical results obtained from the MATLAB simulations for Exercises 1–3. All values reported here were generated directly from the computational scripts and verified for consistency. The raw output file containing these results is included for reference [2].

A. Exercise 1: Aerodynamic Performance Results

- **Q1 – Thrust at 350 km/h (10 km altitude):**

$$T_{\text{req}} = 2891.70 \text{ N}$$

- **Q2 – Minimum Thrust Condition:**

$$C_{L,\min T} = 0.7976, \qquad V_{\min T} = 92.14 \text{ m/s } (331.70 \text{ km/h}),$$

$$T_{\min} = 2875.11 \text{ N}$$

- **Q3 – Minimum Thrust at 7 km Altitude:**

$$V_{\min T}(7 \text{ km}) = 77.17 \text{ m/s } (277.81 \text{ km/h}),$$

$$T_{\min} = 2875.11 \text{ N}$$

(unchanged because minimum thrust depends only on drag balance, not on density).

- **Q4 – Minimum Velocity with $C_{L\max} = 1.2$:**

$$V_{\min} = 75.12 \text{ m/s } (270.43 \text{ km/h}),$$

$$T_{\text{req}}(V_{\min}) = 3118.31 \text{ N}$$

- **Q5 – Maximum Gliding Performance:**

$$\left(\frac{L}{D}\right)_{\max} = 13.29, \qquad R_{\max} = 132.93 \text{ km}$$

B. Exercise 2: Maximum Climb Angle Results

From the MATLAB simulation and velocity sweep:

$$\sin\gamma_{\max} \approx 0.77, \qquad \gamma_{\max} \approx 50^\circ,$$

$$V_{\gamma_{\max}} \approx 72 \text{ m/s}.$$

These results confirm the analytical prediction that maximum climb angle occurs near the velocity minimizing drag per unit lift.

C. Exercise 3: LQR Closed-Loop Performance

- **Controllability:**

$$\text{rank}(Ctrb(A,B)) = 4 \quad \text{(fully controllable)}$$

- **Closed-Loop Poles:** The LQR gain shifts the system poles into the left-half plane, producing fast, well-damped behavior.
- **Initial-Condition Response:** All states converge to zero within approximately 6–8 seconds, satisfying the TP requirement of ≈ 10 s settling time.
- **Control Input Limits:**

$$\max|u| \approx 0.07 \text{ rad} < 0.0873 \text{ rad } (5^\circ)$$

showing that actuator constraints are respected.

These results validate both the aerodynamic models and the LQR controller design.

IX. Conclusion

This expanded study demonstrates the tight integration between aerodynamics and control theory. Analytical and numerical results show excellent agreement across all exercises. The LQR controller provides effective stabilization while respecting actuator limits, illustrating its suitability for remotely piloted aircraft.

References

[1] MATLAB Analytical Output File, Exercise 1–3 Results, self-submitted computation log, 2025.

[2] MATLAB Analytical Output plots, Exercise 1–3 Results,self-submitted, 2025.